Original Article | Neuroimaging and Head & Neck

http://dx.doi.org/10.3348/kjr.2016.17.1.117
pISSN 1229-6929 · eISSN 2005-8330
Korean J Radiol 2016;17(1):117-126

Korean Journal of Radiology
KJR

Pre-Operative Perfusion Skewness and Kurtosis Are Potential Predictors of Progression-Free Survival after Partial Resection of Newly Diagnosed Glioblastoma

Wooyul Paik, MD[1], Ho Sung Kim, MD, PhD[2], Choong Gon Choi, MD[2], Sang Joon Kim, MD[2]

[1]Department of Radiology, Dankook University Hospital, Cheonan 31116, Korea; [2]Department of Radiology and Research Institute of Radiology, University of Ulsan College of Medicine, Asan Medical Center, Seoul 05505, Korea

Objective: To determine whether pre-operative perfusion skewness and kurtosis derived from normalized cerebral blood volume (nCBV) histograms are associated with progression-free survival (PFS) of patients after partial resection of newly diagnosed glioblastoma.

Materials and Methods: A total of 135 glioblastoma patients who had undergone partial resection of tumor (resection of < 50% of pre-operative tumor volume or surgical biopsy) confirmed with immediate postsurgical MRI and examined with both conventional MRI and dynamic susceptibility contrast (DSC) perfusion MRI before the surgery were retrospectively reviewed in this study. They had been followed up post-surgical chemoradiotherapy for tumor progression. Using histogram analyses of nCBV derived from pre-operative DSC perfusion MRI, patients were sub-classified into the following four groups: positive skewness and leptokurtosis (group 1); positive skewness and platykurtosis (group 2); negative skewness and leptokurtosis (group 3); negative skewness and platykurtosis (group 4). Kaplan-Meier analysis and multivariable Cox proportional hazards regression analysis were performed to determine whether clinical and imaging covariates were associated with PFS or overall survival (OS) of these patients.

Results: According to the Kaplan-Meier method, median PFS of group 1, 2, 3, and 4 was 62, 51, 39, and 41 weeks, respectively, with median OS of 82, 77, 77, and 72 weeks, respectively. In multivariable analyses with Cox proportional hazards regression, pre-operative skewness/kurtosis pattern (hazard ratio: 2.98 to 4.64; $p < 0.001$), Karnofsky performance scale score (hazard ratio: 1.04; $p = 0.003$), and post-operative tumor volume (hazard ratio: 1.04; $p = 0.02$) were independently associated with PFS but not with OS.

Conclusion: Higher skewness and kurtosis of nCBV histogram before surgery were associated with longer PFS in patients with newly diagnosed glioblastoma after partial tumor resection.

Index terms: *Brain; Glioblastoma; Surgery; Chemoradiotherapy; Perfusion; Magnetic resonance imaging*

INTRODUCTION

The prognosis of patients with glioblastoma remains poor, with median survival time of 14.6 months after being diagnosed (1). Although multimodal aggressive treatments have been investigated, it has become increasingly important to identify early indicators of progression (2). Currently, efforts have been focused on identifying imaging

Received June 4, 2015; accepted after revision September 22, 2015.
This research was supported by Basic Science Research Program through the National Research Foundation of Korea (NRF) funded by the Ministry of Education, Science and Technology (grant number: NRF-2014R1A2A2A01004937).
Corresponding author: Ho Sung Kim, MD, PhD, Department of Radiology and Research Institute of Radiology, University of Ulsan College of Medicine, Asan Medical Center, 88 Olympic-ro 43-gil, Songpa-gu, Seoul 05505, Korea.
• Tel: (822) 3010-5682 • Fax: (822) 476-0090 • E-mail: radhskim@gmail.com

biomarkers that may affect therapeutic choices and patient outcomes. For example, dynamic susceptibility contrast (DSC) MR imaging can provide a way to characterize tumor biology (3), with measurement of normalized cerebral blood volume (nCBV) being the most widely used hemodynamic variable derived from DSC MR perfusion imaging. Indeed, nCBV has been found to correlate well with glioma grading and tumor microvascular density (4-8).

Histogram analysis has revealed that nCBV is effective for glioma grading by reflecting heterogeneous morphology of high-grade glioma vascularity (8-10). Compared to the hot-spot method, histogram analysis has shown higher inter-observer agreement with comparable diagnostic accuracy (8, 9). On the other hand, it is difficult to establish the influence of increased diagnostic accuracy on clinical outcome. However, high diagnostic accuracy combined with high inter-observer reproducibility are critical criteria for any diagnostic test. One potential advantage of the histogram method is that its results are independent of choice of reference compared to the hot-spot method (7). Therefore, we hypothesized that perfusion skewness and kurtosis derived from nCBV histograms could be used to stratify progression-free survival (PFS) in patients with glioblastoma. The objective of this study was to retrospectively determine whether pre-operative perfusion skewness and kurtosis from semiquantitative histogram analysis of nCBV were associated with PFS of patients with newly diagnosed glioblastoma after partial tumor resection.

MATERIALS AND METHODS

Study Population

Our Institutional Review Board approved this retrospective study and waived the requirement for informed patient consent. Medical records and MR imaging results of 272 patients whose tissue samples obtained via surgery from March 2006 to May 2014 were histologically diagnosed as glioblastoma (World Health Organization grade IV astrocytoma) were retrospectively reviewed. Of these 272 patients, 102 who had gross total tumor resection before concurrent chemoradiotherapy (CCRT) were excluded from this study. In addition, 15 patients who had steroid administration at the time of MR perfusion imaging were excluded. Of the remaining 155 patients, 135 met the following criteria: 1) both conventional and DSC perfusion MRI examinations performed before surgery; 2) residual tumors > 50% of pre-operative tumor volume based on contrast-enhanced T1-weighted MRI obtained after the surgery and before post-surgical CCRT; 3) follow-up MR imaging every 2–3 months after CCRT until tumor progression; and 4) no significant MRI artifact. The 135 patients included 78 males and 57 females whose mean age was 48.4 years (range, 19–83 years). They had a mean follow up time of 47 weeks (range, 42–93 weeks). Preoperative Karnofsky performance scale (KPS) score and extent of surgery (mere surgical biopsy versus therapeutic partial resection) were also assessed from medical records.

Immediate post-operative MRIs were performed following partial tumor resection (also including surgical biopsy) with a mean of 2.2 days interval. Postsurgical CCRT included radiation therapy by administering a total dose of 60 Gy in 2-Gy fractions over a 6-week period and concurrent chemotherapy using temozolomide. Criteria for defining tumor progression included clinical deterioration assessed clinically by a neurooncologist at our institution and radiological progression based on changes in cross-sectional diameters of contrast-enhancing lesion as defined by updated response assessment criteria for high-grade gliomas (11) or confirmed by a second-look operation. PFS and overall survival (OS) were retrospectively calculated based on medical records from partial tumor resection-based pathologic diagnosis to tumor progression and death, respectively.

Conventional MR Imaging

All MR imaging examinations were performed using a 3T system (Achieva; Philips Medical Systems, Best, the Netherlands) with an eight-channel sensitivity encoding head coil. The order of MR imaging acquisition was as follows: T2-weighted imaging, fluid-attenuated inversion recovery imaging, diffusion-weighted imaging, pre-contrast T1-weighted imaging, dynamic contrast-enhanced (DCE) T1-weighted perfusion MR imaging, contrast-enhanced T1-weighted MR imaging, and DSC perfusion MR imaging. DCE perfusion MR imaging was obtained before DSC perfusion MR imaging in order to minimize T1-leakage effect and T2/T2* residual effects by preloading the contrast agent. Transverse T2-weighted fast spin-echo images were obtained with the following parameters: repetition time (TR)/echo time (TE) at 3000/80 msec; field of view at 20 cm; section thickness at 5 mm; matrix at 348 x 270; and acquisition time at 1 minute 54 seconds. Transverse T1-weighted spin-echo images were obtained with the following parameters: TR/TE at 475/10 msec; field of view at 20 cm; section

Korean Journal of Radiology
KJR

thickness at 5 mm; matrix at 256 x 190; and acquisition time at 3 minutes 42 seconds. Diffusion-weighted images were obtained with the following parameters: TR/TE at 3804/46 msec; field of view at 22 cm; section thickness at 5 mm; matrix at 128 x 126; and acquisition time at 1 minute 17 seconds. Contrast-enhanced transverse, sagittal, and coronal T1-weighted spin-echo images were obtained during the administration of a standard dose of 0.1 mmol/kg of gadoterate meglumine (Dotarem; Guerbet, Paris, France) at a rate of 4 mL/s using an MR imaging compatible power injector (Spectris; Medrad, Pittsburgh, PA, USA).

Dynamic Susceptibility-Weighted Contrast-Enhanced MR Imaging

Dynamic susceptibility contrast MR perfusion imaging was performed with gradient-echo echoplanar sequences during the administration of a standard dose of 0.1 mmol/kg of gadoterate meglumine at a rate of 4 mL/sec with an MR imaging-compatible power injector. A bolus of contrast material was followed by injecting 20-mL bolus of saline at the same rate. The following imaging parameters were used for DSC MR perfusion imaging: TR/TE at 1407/40 msec; flip angle at 35°; slice thickness/gap at 5/2 mm; slice number at 20; field of view at 24 cm; and matrix at 128 x 128. The total acquisition time for DSC MR perfusion imaging was 1 minute 30 seconds. DSC MR perfusion imaging was performed by using the same section orientations as those used for conventional MR imaging to covere the entire tumor volume.

Image Processing

Perfusion and conventional MR imaging data were transferred from MR imagers to an independent personal computer for quantitative perfusion analysis. Perfusion parametric maps were obtained using a dedicated software package Nordic ICE (NordicNeuroLab, Bergen, Norway) and an in-house software using Matlab 2010b TM (Mathworks, Natick, MA, USA). A relative CBV map was generated using an established tracer kinetic model applied to first-pass data (12, 13). To reduce the effect of recirculation, we fitted 1/T2* curves to a γ-variate function to approximate the first-pass response as it would appear in the absence of recirculation. As described previously (14), the dynamic curves were corrected mathematically to reduce the effect of contrast agent leakage. After eliminating recirculation and leakage of contrast agent, the relative CBV was computed by numeric integration of the curve. On a pixel-by-pixel basis, the relative CBV maps were normalized by dividing each relative CBV value in a specific section with an unaffected white matter relative CBV value defined by an experienced neuroradiologist. The nCBV maps were displayed as color overlays on post-contrast T1-weighted images.

Image Analyses

Image analyses were performed by using histogram of nCBV derived from DSC perfusion MRI obtained before surgery. Inter-modality co-registrations were performed using a non-linear transformation. For quantitative analysis of the data acquired from DSC MR imaging, the entire volumes of contrast-enhancing lesion were segmented on co-registered contrast-enhanced T1 weighted images using a semi-automated adaptive threshold technique so that all pixels above a threshold value were taken. Therefore, the areas of necrotic and cystic vessels and macro-vessels were excluded. The experienced neuroradiologist approved all region of interests (ROIs).

Histograms were generated by classifying the nCBVs in each ROI into a predefined number of bins (8, 9). The interval between the minimum pixel value and the maximum pixel value was divided into 200 equally spaced bins (8). The number of pixels corresponding to each bin was counted and frequency counts were plotted as a function of bin locations. The range of nCBVs along the x-axis was kept constant between 0 and 10. Since histograms derived from nCBV were often bimodal or skewed, a two-mixture normal distribution was used to provide optimal fitting. Based on visual inspection, this model yielded better fitting curves than either data transformation or higher-level mixtures (15, 16).

The histogram pattern was statistically evaluated for skewness and kurtosis as well as mean, median, and range. Skewness is a measure for the degree of asymmetry of a distribution. A negative skewness indicates an elongated tail on the left side of the mean with most values locating to the right of the mean. A positive skewness indicates an elongated tail on the right side of the mean with most values locating to the left of the mean. Kurtosis is the degree of peak of a distribution. It indicates the relative CBV value at the maximum frequency. Kurtosis for a standard normal distribution is three. For this reason, some sources use the following equation to calculate kurtosis (often referred to as "excess kurtosis"):

$$\text{kurtosis} = \sum Ni = 1(Yi - Y^{-})4 / Ns4 - 3$$

This equation is used so that the standard normal distribution has a kurtosis of zero. In this study, we used the original definition of kurtosis for a standard normal distribution. Therefore, the threshold for leptokurtosis versus platykurtosis was three. Leptokurtosis indicates a sharper peak while platykurtosis indicates a flatter top. The skewness and kurtosis values of our two mixture model were not different from those of the original histogram. Patients were stratified by the histogram patterns of pre-operative tumors into those with positive skewness and leptokurtosis (group 1), those with positive skewness and platykurtosis (group 2); those with negative skewness and leptokurtosis (group 3); and those with negative skewness and platykurtosis (group 4).

Statistical Analyses

Clinical and conventional imaging parameters among the four groups were compared by using analysis of variance (ANOVA) for continuous variables and chi-square test for categorical variables. Quantitative histogram parameters among the four groups were compared by using ANOVA. Multiple comparisons were corrected by using Bonferroni correction. Kaplan-Meier method was used to calculate median PFS and OS. Cox proportional hazards regression was performed to assess the effect of patient age, gender, KPS score, pre-operative tumor size, surgical extent (biopsy versus partial resection), post-operative tumor size, radiation dose at CCRT, and skewness/kurtosis pattern on PFS and OS. Patients who remained alive at analysis were considered censored on the date of last follow-up visit. All statistical analyses were performed using SPSS for Windows, version 14.0 (SPSS Inc., Chicago, IL, USA). Statistical significance was considered when p value was less than 0.05.

RESULTS

Clinical Characteristics and Histogram Patterns of Study Patients

The clinical characteristics of study patients in each group according to the histogram pattern (skewness/kurtosis) are summarized in Table 1. Of the 135 tumors investigated, 22 were classified into group 1, 58 into group 2, 29 into group 3, and 26 into group 4. The four groups were overall well-balanced in terms of clinical and conventional imaging parameters. More patients in group 1 had longer (corrected $p = 0.045$) mean follow-up periods. Examples of the histogram patterns of pre-operative glioblastomas are shown in Figures 1-3. The mean time for post processing of an MR perfusion histogram was 7 minutes and 22 seconds. The mean values of histogram parameters derived from pre-operative tumor nCBV in each group are summarized in Table 2. All quantitative histogram values including range, median, mean, skewness, and kurtosis were significantly (corrected $p < 0.001$) different among the four groups.

Histogram Patterns versus PFS and OS

Kaplan-Meier curves of PFS for the four histogram patterns are shown in Figure 4A. Median PFSs of group 1, 2, 3, and 4 were 62, 51, 39, and 41 weeks, respectively. The Kaplan-Meier curves of OS for the four histogram patterns are shown in Figure 4B. Median OS times of group 1, 2, 3, and 4 were 82, 77, 77, and 72 weeks, respectively.

Multivariate Analyses for PFS and OS

Cox proportional hazards regression indicated that the pre-operative tumor perfusion histogram pattern (skewness/kurtosis) (hazard ratio of 2.98 for group 1 versus group 2, $p < 0.001$; hazard ratio of 4.38 for group 1 versus group 3,

Table 1. Comparison of Clinical and Conventional Imaging Data among Study Subgroups

Characteristics	Group 1 (n = 22)	Group 2 (n = 58)	Group 3 (n = 29)	Group 4 (n = 26)	Corrected *P*
Age*, years	42.4 ± 5.7	50.3 ± 7.1	48.6 ± 6.3	49.0 ± 6.9	0.25
Male gender (%)	11 (50.0)	33 (56.9)	20 (69.0)	14 (53.8)	0.99
KPS*	87.3 ± 5.7	86.9 ± 5.1	91.7 ± 5.5	90.0 ± 4.9	0.40
Preoperative tumor size*, cm^3	32.9 ± 15.7	36.4 ± 14.3	39.7 ± 17.1	42.8 ± 12.9	0.55
Partial resection (vs. biopsy) (%)	16 (72.7)	46 (79.3)	22 (75.9)	12 (46.2)	0.10
Postoperative tumor size*, cm^3	23.6 ± 11.3	28.6 ± 12.1	31.1 ± 11.5	33.9 ± 9.5	0.23
Radiation dose at CCRT*, Gy	58.7 ± 0.4	59.1 ± 0.5	58.6 ± 0.5	59.2 ± 0.3	0.99
Adjuvant temocycles*	4.2 ± 0.7	5.2 3 ± 0.5	5.2 ± 0.4	5.3 ± 0.3	0.25
Follow-up periods*, weeks	71.7 ± 15.9	54.0 ± 17.1	52.5 ± 16.5	51.7 ± 14.1	0.045

p values were calculated by ANOVA for continuous variables and chi-square test for categorical variables and corrected for multiple comparisons by using Bonferroni correction. *Data are mean ± standard deviation. ANOVA = analysis of variance, CCRT = concurrent chemoradiotherapy, KPS = Karnofsky performance scale

Korean Journal of Radiology
KJR

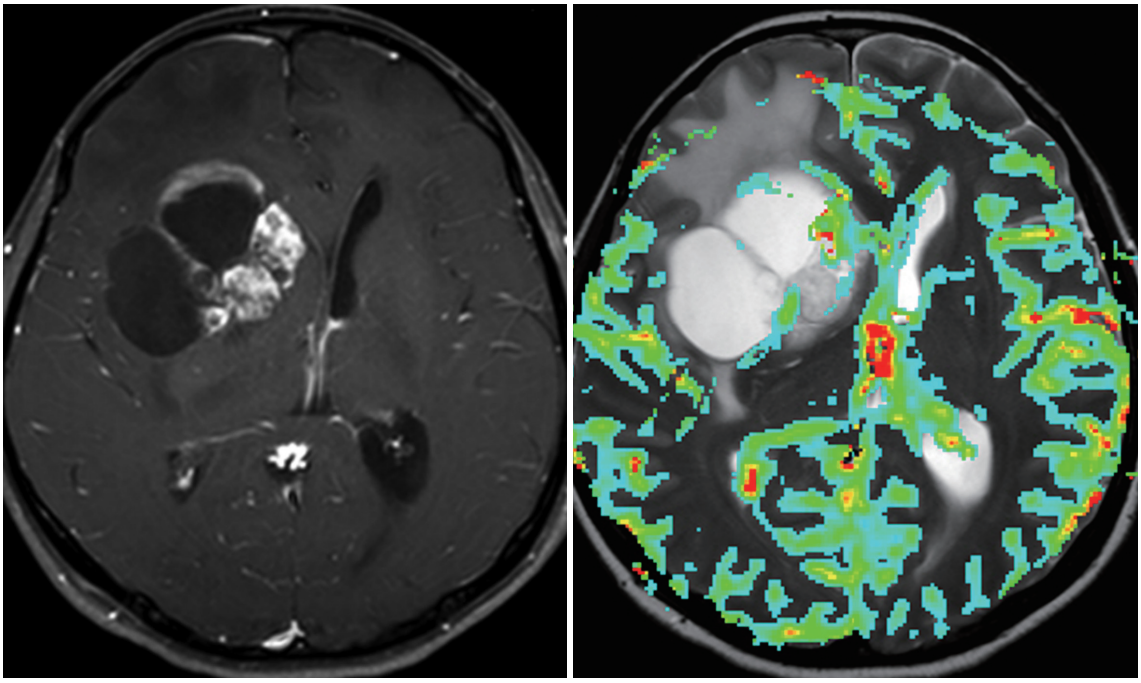

A B

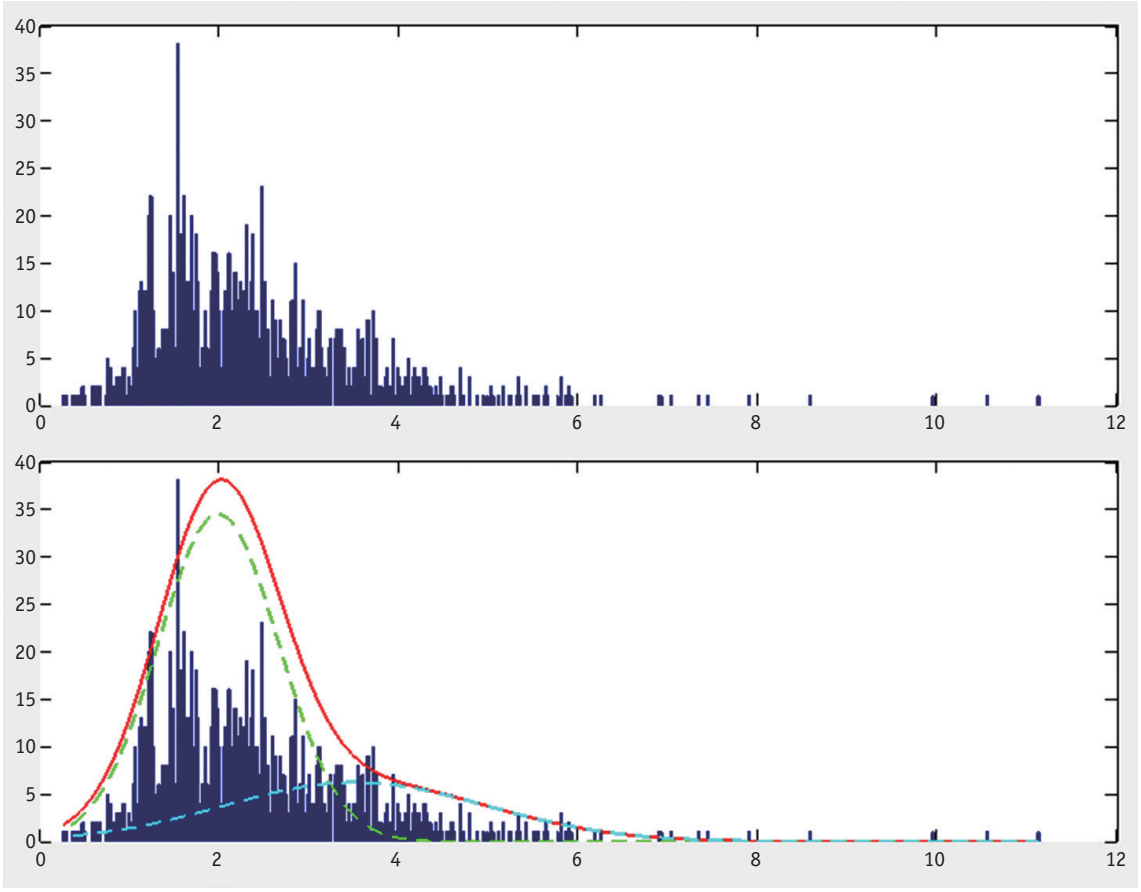

C

Fig. 1. Example of group 1 patient with positive skewness and leptokurtosis.
A. 45-year-old man with pathologically proven glioblastoma. Contrast-enhanced T1-weighted image showing contrast-enhancing mass in right frontal lobe. **B.** MR perfusion image showing increased nCBV in corresponding contrast-enhancing-lesion. **C.** Histogram derived from nCBV had positive skewness and leptokurtosis (skewness = 1.14, kurtosis = 4.32). nCBV = normalized cerebral blood volume

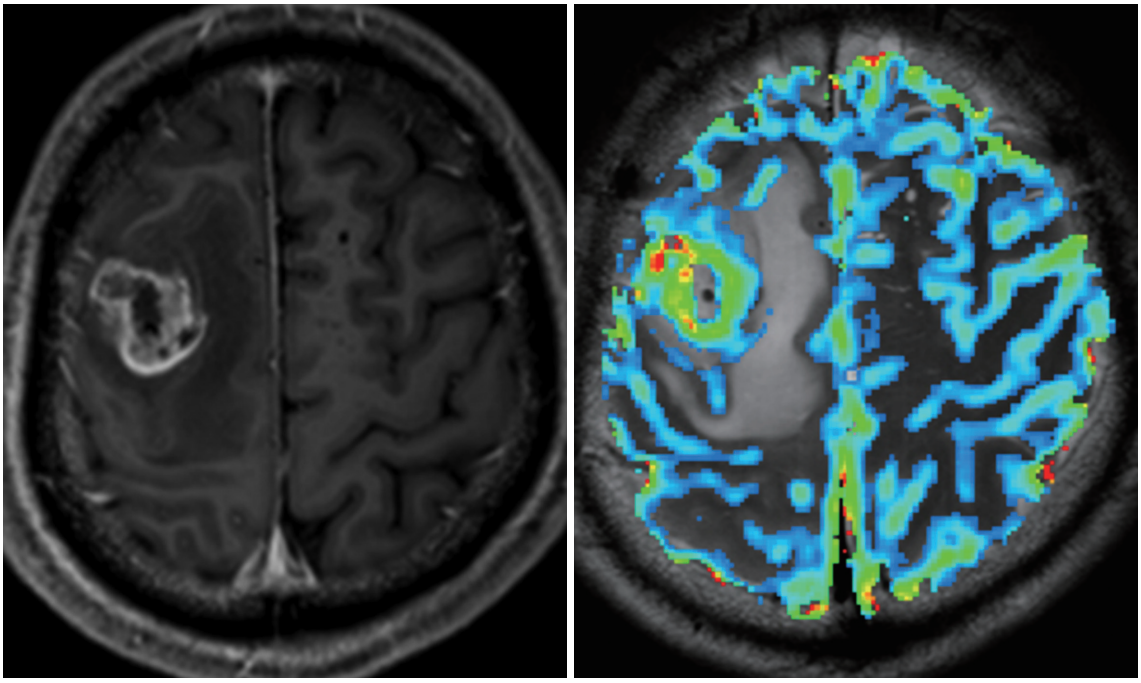

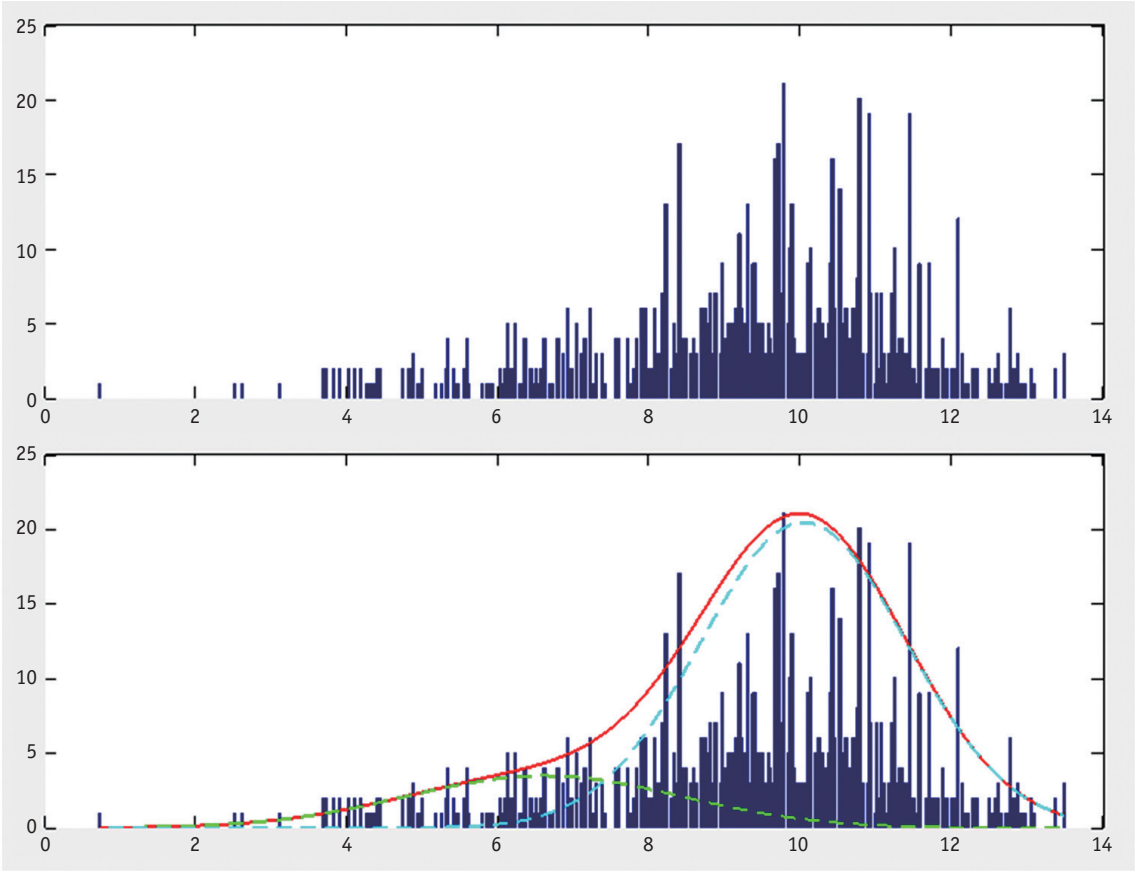

Fig. 2. Example of group 3 patient with negative skewness and leptokurtosis.
A. 54-year-old man with pathologically proven glioblastoma. Contrast-enhanced T1-weighted image showing contrast-enhancing mass in right frontal lobe. **B.** MR perfusion image showing increased nCBV in corresponding contrast-enhancing-lesion. **C.** Histogram derived from nCBV had negative skewness and leptokurtosis (skewness = -0.76, kurtosis = 3.52). nCBV = normalized cerebral blood volume

Korean Journal of Radiology
KJR

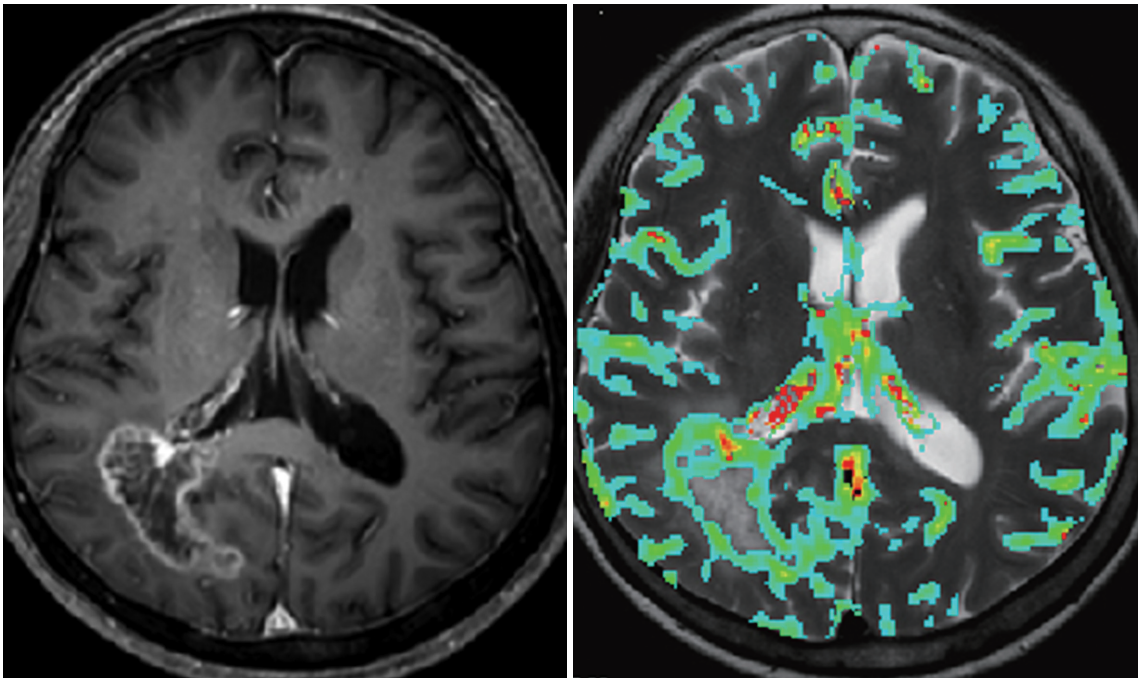

A B

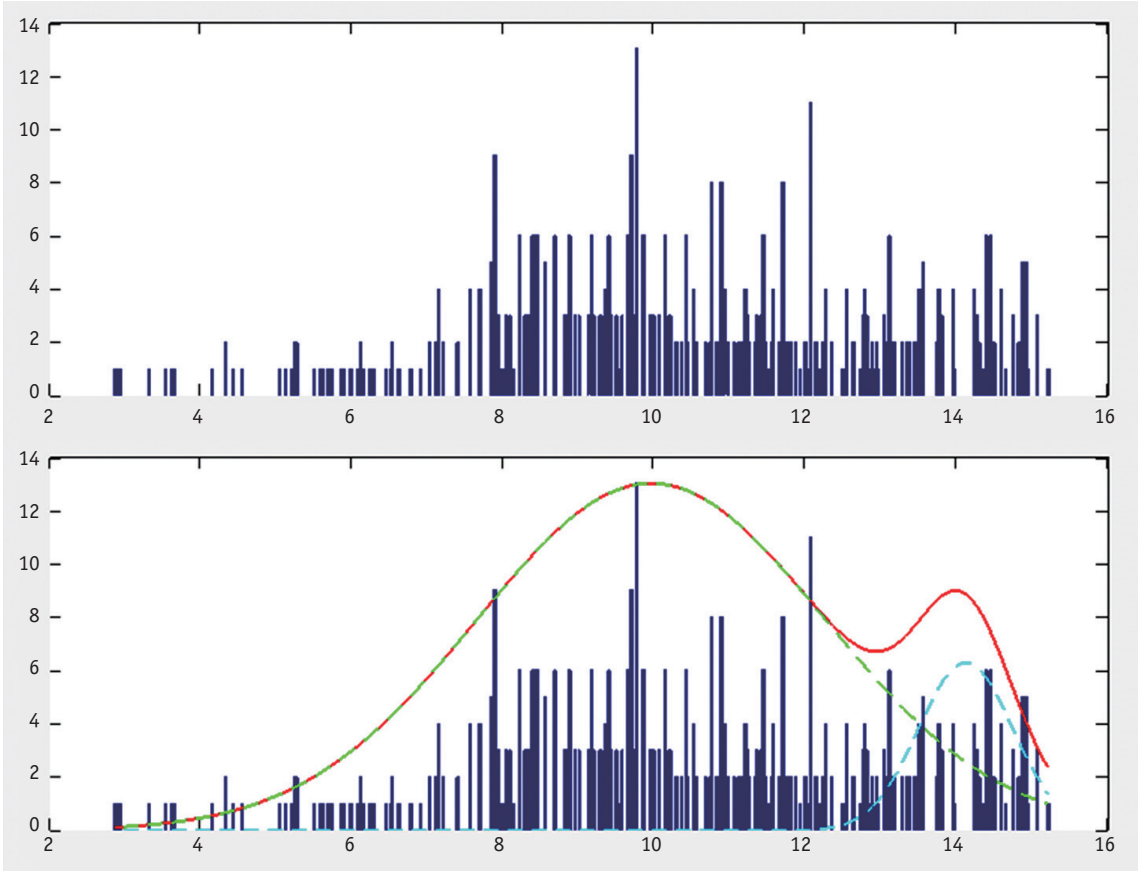

C

Fig. 3. Example of group 4 patient with negative skewness and platykurtosis.
A. 66-year-old woman with pathologically proven glioblastoma. Contrast-enhanced T1-weighted image showing contrast-enhancing mass in right frontal lobe. **B.** MR perfusion image showing increased nCBV in corresponding contrast-enhancing-lesion. **C.** Histogram derived from nCBV had negative skewness and platykurtosis (skewness = -0.05, kurtosis = 2.31). nCBV = normalized cerebral blood volume

$p < 0.001$; hazard ratio of 4.64 for group 1 versus group 4, $p < 0.001$) was an independent predictor for PFS, but not for OS. The KPS score (hazard ratio of 1.04, $p = 0.003$) and post-operative tumor size (hazard ratio of 1.04, $p = 0.02$) were also independent predictors for PFS, but not for OS. Whereas age, gender, post-operative tumor size, surgical

Table 2. Mean Quantitative Values of Histogram Parameters Derived from Normalized Cerebral Blood Volume in Subgroups by Skewness/Kurtosis Pattern

Histogram Parameters	Group 1 (n = 22)	Group 2 (n = 58)	Group 3 (n = 29)	Group 4 (n = 26)	Corrected *P*
Range	7.76 ± 2.16	7.79 ± 2.21	9.87 ± 1.92	9.07 ± 2.34	< 0.001
Median	3.89 ± 1.37	4.03 ± 1.53	8.23 ± 1.97	8.12 ± 2.01	< 0.001
Mean	4.14 ± 1.42	4.22 ± 1.51	8.11 ± 1.92	8.29 ± 1.99	< 0.001
Skewness	0.98 ± 0.17	0.52 ± 0.15	-0.61 ± 0.16	-0.54 ± 0.14	< 0.001
Kurtosis	3.76 ± 0.93	2.07 ± 0.92	3.59 ± 0.97	2.01 ± 0.83	< 0.001

Data are mean ± standard deviation. *p* values were calculated by ANOVA and corrected for multiple comparisons by using Bonferroni correction. ANOVA = analysis of variance

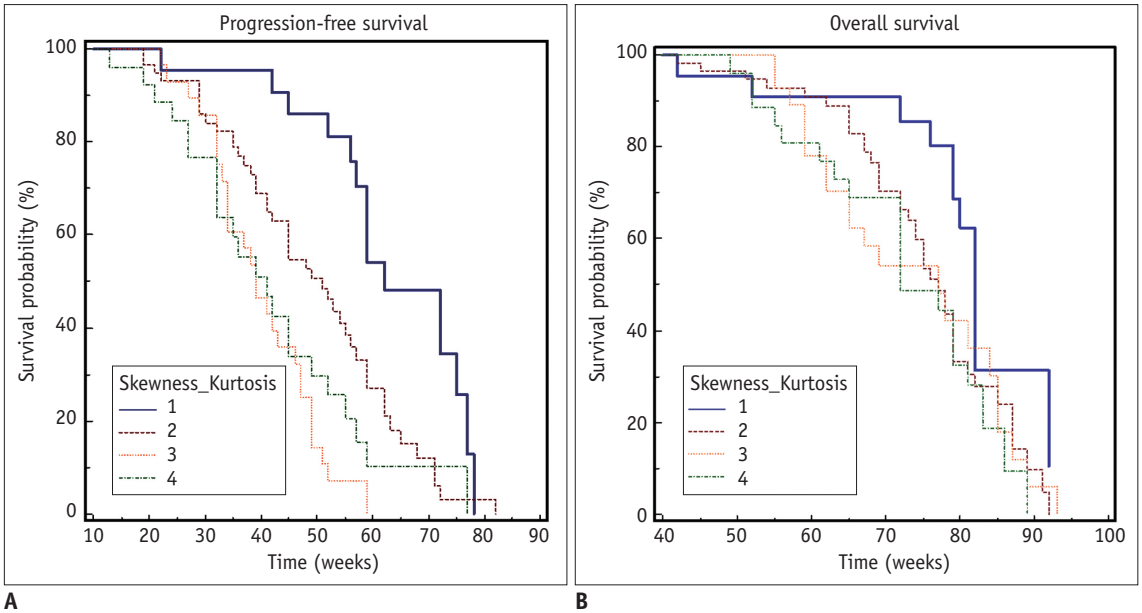

A B

Fig. 4. Kaplan-Meier survival curves of patients stratified by perfusion skewness and kurtosis for progression-free survival (A) and overall survival (B). Patients were stratified by histogram patterns of pre-operative tumors into those with positive skewness and leptokurtosis (group 1), those with positive skewness and platykurtosis (group 2), those with negative skewness and leptokurtosis (group 3), and those with negative skewness and platykurtosis (group 4). Progression-free survival and overall survival tended to be longer in group 1.

Table 3. Clinical and Imaging Variables Associated with Progression-Free Survival and Overall Survival in Patients with Glioblastoma

Variables	Progression-Free Survival		Overall Survival	
	Hazard Ratio (95% CI)	*P*	Hazard Ratio (95% CI)	*P*
Age, years	0.99 (0.98–1.01)	0.57	1.01 (0.99–1.03)	0.21
Male gender	0.80 (0.53–1.21)	0.20	0.87 (0.54–1.38)	0.55
KPS score	1.04 (1.01–1.07)	0.003	1.00 (0.97–10.3)	0.92
Preoperative tumor size, cm^3	0.98 (0.95–1.01)	0.14	1.01 (0.98–1.04)	0.61
Biopsy (vs. partial tumor resection)	1.44 (0.90–2.33)	0.13	0.99 (0.60–1.65)	0.99
Postoperative tumor size, cm^3	1.04 (1.01–1.08)	0.02	0.99 (0.96–1.03)	0.83
Radiation dose at CCRT, Gy	0.93 (0.84–1.03)	0.16	1.01 (0.90–1.13)	0.93
Skewness/kurtosis group 2 (vs. group 1)	2.98 (1.56–5.67)	< 0.001	1.51 (0.78–2.93)	0.22
Skewness/kurtosis group 3 (vs. group 1)	4.38 (2.12–9.05)	< 0.001	1.93 (0.90–4.15)	0.10
Skewness/kurtosis group 4 (vs. group 1)	4.64 (2.18–9.92)	< 0.001	2.06 (0.97–4.37)	0.06

CCRT = concurrent chemoradiotherapy, CI = confidence interval, KPS = Karnofsky performance scale

Korean Journal of Radiology
KJR

extent, and radiation dose at CCRT were not independent predictors for PFS or OS (Table 3).

DISCUSSION

Our results revealed that both skewness and kurtosis of nCBV histograms obtained from presurgical MRI were associated with PFS of patients with newly diagnosed glioblastoma after partial tumor resection. Glioblastomas with negative skewness and platykurtosis showed significantly more rapid time to progression than those with positive skewness and leptokurtosis. A longer time to progression was associated with most nCBV values that were lower with narrower and more peaked shape of the histogram, reflecting more homogeneous tumor composition. Although our results revealed that histogram patterns could predict PFS, no correlation between histogram pattern and OS was found. Many clinical, surgical, and therapy-associated factors may affect OS. In addition, the censoring of 36 patients might have affected the true OS.

A previous study (9) has found that the standard deviation of relative CBV reflecting the dispersion of data around the arithmetic mean has the highest correlation with glioma grade, indicating the heterogeneous biological nature of high-grade gliomas. However, these measurements showed reduced precision and validity because our data did not have a normal distribution. Measuring the degree of histogram asymmetry and peaking using statistical parameters of skewness and kurtosis yielded results similar to a real clinical setting. Moreover, although semi-quantitative analysis requires a reasonable time for post-processing and image analysis, it has clinical implications to noninvasively identify and predict patient outcomes. An outcome-based classification would be of greater value because it will allow the use of potential prognostic factors to tailor individual therapy regimens (17).

We found that tumors with slower progression had significantly lower means and smaller ranges on nCBV histograms. These findings were in accordance with previous results showing that higher tumor fractions were associated with higher peak height and wider range (6). Such results might be due to heterogeneous expression of aggressive cellular features. Broadly elevated microvascular density has been shown to correlate with elevated tumor cellularity, malignant progression, and extensive tumor invasiveness, resulting in poor prognostic outcomes (18).

Several studies have investigated the prognostic value of tumor CBV on survival in patients with glioma and found correlations between tumor CBV and patient outcomes (2, 3, 19-21). However, these studies used median CBV (2, 19), maximal CBV (21), or ROI-based techniques of relative CBV measurements (3, 17, 20). They failed to assess the heterogeneous perfusion characteristics of high grade gliomas. We used skewness and kurtosis from histograms of nCBV as markers of tumor perfusion degree and heterogeneity, respectively. In terms of PFS, group 3 and group 4 that shared the skewness criteria with different kurtosis had similar PFS, indicating that the difference of kurtosis might be associated with PFS stratification more in the positive skewness group than in the negative skewness group.

This study had several limitations. First, the sample size of each group was different. Although OS tended to be longer in group 1, the difference was not statistically significant. This might be due to the small number of patients in this group. More even sample sizes might have strengthened the statistical power of our findings. Second, it was challenging to define the entire tumor volume using the histogram method because gliomas are infiltrating tumors with indistinct borders beyond radiologic margins (22). However, results from a previous study (8) have shown that variations among observers caused by imperfect tumor delineation are relatively unimportant although a large number of data points are included in each histogram. Lastly, we excluded glioblastoma patients with gross-total tumor resection who seemed to be unsuitable for pre-operative tumor perfusion evaluation. However, homogeneous group of patients with biopsy or partial tumor resection enabled us to assess the association between the tumor perfusion characteristics and treatment response to CCRT more reliably. Moreover, pre-operative tumor perfusion evaluation using DSC MR imaging is more appropriate than post-operative and pre-CCRT study because DSC MR imaging could be sensitive to susceptibility artifact associated with post-operative hemorrhage or surgical material.

In conclusion, higher skewness and kurtosis of nCBV histogram before surgery were associated with longer PFS of patients with newly diagnosed glioblastoma after partial tumor resection. Therefore, pre-operative perfusion skewness and kurtosis derived from nCBV might be used as a potential predictor of PFS of these patients.

REFERENCES

1. Smith JS, Jenkins RB. Genetic alterations in adult diffuse glioma: occurrence, significance, and prognostic implications. *Front Biosci* 2000;5:D213-D231
2. Cao Y, Tsien CI, Nagesh V, Junck L, Ten Haken R, Ross BD, et al. Survival prediction in high-grade gliomas by MRI perfusion before and during early stage of RT [corrected]. *Int J Radiat Oncol Biol Phys* 2006;64:876-885
3. Law M, Young RJ, Babb JS, Peccerelli N, Chheang S, Gruber ML, et al. Gliomas: predicting time to progression or survival with cerebral blood volume measurements at dynamic susceptibility-weighted contrast-enhanced perfusion MR imaging. *Radiology* 2008;247:490-498
4. Jahng GH, Li KL, Ostergaard L, Calamante F. Perfusion magnetic resonance imaging: a comprehensive update on principles and techniques. *Korean J Radiol* 2014;15:554-577
5. Lee EK, Choi SH, Yun TJ, Kang KM, Kim TM, Lee SH, et al. Prediction of response to concurrent chemoradiotherapy with temozolomide in glioblastoma: application of immediate post-operative dynamic susceptibility contrast and diffusion-weighted MR imaging. *Korean J Radiol* 2015;16:e148
6. Kim HS, Kim JH, Kim SH, Cho KG, Kim SY. Posttreatment high-grade glioma: usefulness of peak height position with semiquantitative MR perfusion histogram analysis in an entire contrast-enhanced lesion for predicting volume fraction of recurrence. *Radiology* 2010;256:906-915
7. Emblem KE, Bjornerud A. An automatic procedure for normalization of cerebral blood volume maps in dynamic susceptibility contrast-based glioma imaging. *AJNR Am J Neuroradiol* 2009;30:1929-1932
8. Emblem KE, Nedregaard B, Nome T, Due-Tonnessen P, Hald JK, Scheie D, et al. Glioma grading by using histogram analysis of blood volume heterogeneity from MR-derived cerebral blood volume maps. *Radiology* 2008;247:808-817
9. Law M, Young R, Babb J, Pollack E, Johnson G. Histogram analysis versus region of interest analysis of dynamic susceptibility contrast perfusion MR imaging data in the grading of cerebral gliomas. *AJNR Am J Neuroradiol* 2007;28:761-766
10. Emblem KE, Scheie D, Due-Tonnessen P, Nedregaard B, Nome T, Hald JK, et al. Histogram analysis of MR imaging-derived cerebral blood volume maps: combined glioma grading and identification of low-grade oligodendroglial subtypes. *AJNR Am J Neuroradiol* 2008;29:1664-1670
11. Wen PY, Macdonald DR, Reardon DA, Cloughesy TF, Sorensen AG, Galanis E, et al. Updated response assessment criteria for high-grade gliomas: response assessment in neuro-oncology working group. *J Clin Oncol* 2010;28:1963-1972
12. Rosen BR, Belliveau JW, Vevea JM, Brady TJ. Perfusion imaging with NMR contrast agents. *Magn Reson Med* 1990;14:249-265
13. Ostergaard L, Weisskoff RM, Chesler DA, Gyldensted C, Rosen BR. High resolution measurement of cerebral blood flow using intravascular tracer bolus passages. Part I: Mathematical approach and statistical analysis. *Magn Reson Med* 1996;36:715-725
14. Boxerman JL, Schmainda KM, Weisskoff RM. Relative cerebral blood volume maps corrected for contrast agent extravasation significantly correlate with glioma tumor grade, whereas uncorrected maps do not. *AJNR Am J Neuroradiol* 2006;27:859-867
15. Pope WB, Kim HJ, Huo J, Alger J, Brown MS, Gjertson D, et al. Recurrent glioblastoma multiforme: ADC histogram analysis predicts response to bevacizumab treatment. *Radiology* 2009;252:182-189
16. Nowosielski M, Recheis W, Goebel G, Güler O, Tinkhauser G, Kostron H, et al. ADC histograms predict response to anti-angiogenic therapy in patients with recurrent high-grade glioma. *Neuroradiology* 2011;53:291-302
17. Bisdas S, Kirkpatrick M, Giglio P, Welsh C, Spampinato MV, Rumboldt Z. Cerebral blood volume measurements by perfusion-weighted MR imaging in gliomas: ready for prime time in predicting short-term outcome and recurrent disease? *AJNR Am J Neuroradiol* 2009;30:681-688
18. Barajas RF Jr, Hodgson JG, Chang JS, Vandenberg SR, Yeh RF, Parsa AT, et al. Glioblastoma multiforme regional genetic and cellular expression patterns: influence on anatomic and physiologic MR imaging. *Radiology* 2010;254:564-576
19. Oh J, Henry RG, Pirzkall A, Lu Y, Li X, Catalaa I, et al. Survival analysis in patients with glioblastoma multiforme: predictive value of choline-to-N-acetylaspartate index, apparent diffusion coefficient, and relative cerebral blood volume. *J Magn Reson Imaging* 2004;19:546-554
20. Law M, Oh S, Babb JS, Wang E, Inglese M, Zagzag D, et al. Low-grade gliomas: dynamic susceptibility-weighted contrast-enhanced perfusion MR imaging--prediction of patient clinical response. *Radiology* 2006;238:658-667
21. Lev MH, Ozsunar Y, Henson JW, Rasheed AA, Barest GD, Harsh GR 4th, et al. Glial tumor grading and outcome prediction using dynamic spin-echo MR susceptibility mapping compared with conventional contrast-enhanced MR: confounding effect of elevated rCBV of oligodendrogliomas [corrected]. *AJNR Am J Neuroradiol* 2004;25:214-221
22. Price SJ, Jena R, Burnet NG, Hutchinson PJ, Dean AF, Peña A, et al. Improved delineation of glioma margins and regions of infiltration with the use of diffusion tensor imaging: an image-guided biopsy study. *AJNR Am J Neuroradiol* 2006;27:1969-1974